Dalton Transactions

Accepted Manuscript

ROYAL SOCIETY OF CHEMISTRY

www.rsc.org/dalton

IL and LTTM based on amine alcohol were prepared and solitonic proton charge transfer supposed to be in LTTM

Journal Name

ARTICLE

Solutions of complex copper salts in LTTM

Maxim A. Zakharov,[a] Gennady V. Fetisov,[a] Alexei A. Veligzhanin,[b] Michael A. Bykov,[a] Ksenia A. Paseshnichenko,[a] Sergei F. Dunaev[a] and Leonid A. Aslanov[a]*

Received 00th January 20xx,
Accepted 00th January 20xx

DOI: 10.1039/x0xx00000x

www.rsc.org/

The structure and properties of diethanolamine complexes of copper(II) triflates dissolved in excess of diethanolamine (DH_2) were studied. The copper containing substance was found to be a solution of copper(II) complex salt $[Cu^{2+}DH_2(DH^-)]OTf^-$ in LTTM composition $[(DH_2)_4H^+](OTf^-)$, where LTTM = low-transition-temperature mixture, OTf^- = trifate anion. According to the EXAFS data, coordination number of copper(II) atoms in solution does not exceed 4. Addition of even negligible amounts of acid significantly changes DH_2 volatility and decomposition conditions.

Introduction

Ionic liquids (ILs) are intensively studied due to variety and specificity of their properties opening wide perspectives of their application. Beginning from 2003[1], deep eutectic solvents (DES)[2–5] are used as well. DES are more convenient than ILs: they are cheaper and easier in production, their properties being very close to those of ILs. Later a special group of solvents, low-transition-temperature mixtures (LTTMs)[6], was introduced. These solvents have no eutectic point and that is why differ from DES.

Recently, a new group of ionic liquids, MetILs[7–10] (ionic liquid with metal coordination cation) with transition metal ions as coordination centers and aminoalcohols as ligands, was suggested. MetILs are very attractive for application in molecular magnets[11–14], galvanoplastics[15–17] and for production of novel electric accumulators[18]. They have two advantages: low price and high metal concentration which cannot be obtained in solutions of salts[19–20].

Earlier it was shown[21] that diethanolamine (DH_2) and copper ions form complexes $[CuDH_2]^{2+}$ at pH 6.0–6.4, but at pH 7.2–11.0 the OH groups are deprotonated, and that is why $[CuDH_2DH]^+$ cations or neutral $[Cu(DH)_2]$ complexes are formed with increasing pH.

Tauler and co-workers[22] found that in the pH range 3–12 only mononuclear complexes with the chelating diethanolamine ligands are formed in aqueous solutions. However, binuclear Cu(II) complexes were obtained and their crystal structures solved[23–24]. In these complexes, the deprotonated hydroxyl groups form bridges between copper atoms. The earlier data on Cu(II) complex formation with diethanolamine are summarized in a review.[25]

There are a lot of interesting findings[7–10] related with synthesis, structure and properties of MetILs with a general formula $MA_2 \cdot 6L$, where M = Fe(III), Cu(II), Mn(II), Zn(II), A = $CF_3SO_3^-$ = OTf (triflate anion), $N(SO_2CF_3)_2^-$ = NTf_2^- (bis(trifluoromethylsulfonyl)imide), $CH_3(CH_2)CH(C_2H_5)COO^-$ = EHN (2-ethylhexanoate ion), L = DH_2 or EH (ethanolamine). All the obtained MetILs are considered to be individual coordination compounds rather than solutions of transition metal salts or their complexes in excess of ligand[7–10]. In all MetILs coordination number of metal atom is 6.

Crystals of $[CuDH_2DH]OTf$ were isolated from MetILs of the composition $Cu(OTf)(EHN) \cdot 6DH_2$. Their crystal structure was solved and it appeared that[9]: (1) only two DH_2 of six are in the inner coordination sphere of Cu atom; (2) both DH_2 are chelating ligands forming coordination bonds *via* the N and O atoms; (3) one of the hydroxyl groups bound to Cu atom is deprotonated. It should be noted that deprotonation of the hydroxyl groups in the presence of amines usually yields metal alcoholates[27–28]; ethanolamine forms alcoholates under the same conditions as alcohols[29] and can form alcoholates even without addition of secondary and tertiary amines, yielding the ammonium tautomer[25]. And the last (4) but not least: Cu(II) coordination number is 4 + 2, what is typical of Cu(II) cations. Based on the above mentioned crystal structure, a hypothesis that $Cu(OTf)(EHN) \cdot 6DH_2$ and $Cu(OTf)_2 \cdot 6DH_2$ can be solutions of Cu(II) complex salt in DES or LTTM must not be excluded. This hypothesis is tested in the present work.

The only problem not considered in [7–10] is localization of the hydroxyl group proton splitted out due to complex formation. A concept of "proton wires" or "proton pumps" is widely developed in the modern biology. This concept mainly considers migration of protons *via* the chains of water molecules with formation of oxonium ions, although special attention is also paid to ammonium cations and

[a] *Department of Chemistry, Lomonosov Moscow State University, Moscow, 119991 Russian Federation. E-mail: aslanov@struct.chem.msu.ru; Tel: +7 495 9391327; www: http://www.chem.msu.su/ .*
[b] NRC Kurchatov Institute, Kurchatov Square 1, Moscow, 123182 *Russian* Federation

hydrogen bonds formed between them and N-heterocycles or amino groups[31–34]. A model of the proton transport *via* the chain of ammonia molecules[35] considers a block $H_3N…H^+…NH_3$ as the central unit. This block has been found in crystalline state[36] and is analogous to the well-studied stable ion $H_5O_2^+$ in which a proton is coordinated by two oxygen atoms[26]. Crystal structures of more complex aggregates of ammonium cations and ammonia molecules with short and strong hydrogen bonds are also known[37]. The enthalpy of reaction in gaseous phase

$$NH_4^+(NH_3)_n + NH_3 = NH_4^+(NH_3)_{n+1}$$

is ~ 17 kcal/mol for n = 0, slightly lower than 17 kcal/mol for n = 1 and ~ 15 kcal/mol for n = 2.[38]

According to [26], a proton can bind to the O atoms of hydroxyl groups in the presence of super acids. Under such conditions[39], protons form a dynamical system composed of O–H σ-bonds and O…H hydrogen bonds, σ-bonds and hydrogen bonds can interchange places; this is equal to a rapid migration of charge of the super acid proton between all the ligands. A similar dynamical system is supposed to exist at the super- acidic proton addition to primary and secondary amines, because the electron affinity of ammonia and amines is higher than that of water, alcohols and ethers[40]. Volatility of ligands is decreased in the presence of onium salts, and this is one of the key properties of $Cu(OTf)_2 \cdot 6DH_2$ and DES.

The structures of metal complexes in crystals and liquids can be different, that is why we have studied coordination numbers of metal atoms in $Cu(OTf)_2 \cdot 6DH_2$ compared with some other compounds (see Table 1) by EXAFS and also investigated the properties of DH_2–HOTf system.

Experimental section

Materials and Reagents

Reagents used in the present research $HN[(CH_2)_2OH]_2$ (99%, Acros), $H_2N(CH_2)_6OH$ (97%, Aldrich), $H_2N(CH_2)_2OH$ (99%, Sigma-Aldrich), $Cu_2(OH)_2CO_3$ (95%, Aldrich), $Fe(NO_3)_3 \cdot 9H_2O$ (98%, Sigma-Aldrich), $FeCl_3 \cdot 6H_2O$ (97%, Sigma-Aldrich), CF_3SO_3H (99%, Acros) were taken without further purification.

Synthesis

The samples investigated in this research are listed in Table 1 with their designations and chemical formulae. These compositions were synthesized in two stages. In the first stage, Cu(II) triflate[41] and Fe(III) triflate[42] were prepared by the known methods.

In the second stage, the final compositions were obtained by mixing the corresponding metal triflate and aminoalcohol. Full details are given in the Supplementary Materials.

Table 1. The list of investigated samples.

Designation	Chemical composition
$Cu(OTf)_2 \cdot 6EH$	$Cu(CF_3SO_3)_2 \cdot 6H_2N(CH_2)_2OH$
$Cu(OTf)_2 \cdot 6HH$	$Cu(CF_3SO_3)_2 \cdot 6HN(CH_2)_6OH$
$Fe(OTf)_3 \cdot 6HH$	$Fe(CF_3SO_3)_3 \cdot 6HN(CH_2)_6OH$
$Fe(OTf)_3 \cdot 6DH_2$	$Fe(CF_3SO_3)_3 \cdot 6HN((CH_2)_2OH)_2$
$Cu(OTf)_2 \cdot 6DH_2$	$Cu(CF_3SO_3)_2 \cdot 6HN((CH_2)_2OH)_2$

Analytical methods

Differential thermal analysis – Thermogravimetry – Mass-spectrometry (DTA-TG-MS). Simultaneous thermogravimetry and analysis of the decomposition products by mass spectrometry were performed using a Netzsch STA-409 PC/PG analyzer, heating rate of 5 °C/min, argon stream 40 l/min.

Differential scanning calorimetry (DSC). Samples were analyzed using a Netzsch DSC-204 F1 analyzer in a high purity nitrogen flow 40 ml/min with the standard aluminum cells, temperature range 130–60 °C, heating and cooling rates 5 °C/min with temperature detection error 0.1°.

Infrared spectroscopy. The FTIR spectra in the wave number range of 500-4000 $см^{-1}$ were recorded using the Perkin-Elmer SPECTRUM ONE FTIR spectrometer.

MALDI mass spectra were recorded using a Bruker Autoflex II MALDI-TOF MS. The spectrometer (FWHM resolution 18000) had a nitrogen laser with wavelength 337 nm and a time of flight mass analyzer operating in the reflection mode. Samples were applied on a polished stainless steel substrate. The spectrum was recorded in the positive ion mode. The resulting spectrum was the sum of 300 spectra obtained at different points of a specimen. Anthracene (Acros, 99%) served as a matrix.

EXAFS spectroscopy for local structure analysis

Local structure of liquids was studied by EXAFS spectroscopy within the energy range about X-ray absorption K-edge of metal atoms in composition of the investigated substances. The modern theoretical and practical basics of this method can be found, for example, in a book by Fetisov[43], Chapter 5. More detailed description of structural analysis by XAFS methods including the detailed instruction is given by G. Bunker in the Manual Guide.[44]

The X-ray absorption spectra around K-edges of the metals present in the investigated liquids have been recorded in the transmission mode on the X-ray beam line "The Structural Materials Science"[45] (bending magnet source, "Siberia-2" storage ring at Kurchatov Synchrotron Radiation Source (KSRS), Moscow, Russia) equipped with a

Si(111) channel-cut monochromator having energy resolution $\Delta E/E$ ~ 2×10^{-4}. The ring was operating at 2.5 GeV with the electron currents decaying from 45 to 35 mA. The size of the SR beam at the sample location was 1 mm(V) × 2 mm(H). EXAFS spectra were recorded in transmission mode using ionization chambers filled with air. The ionization current of the chambers was measured with Keithley 6487 picoampermeters. We used three ionization chambers: two of them measured the intensity of the primary (I_0) and transmitted through the sample (I_t) radiation beams. The sample was located between these ionization chambers on the path of the primary beam. The third chamber measured the intensity (I_s) of the SR beam passing through the reference sample which was used for absolute calibration of photon energy. The foil made of metal in the composition of investigated liquid served as the reference.

The absorption spectra of the samples were recorded step-by-step within energy interval from -170 to +800 eV relative the K-edge of absorbing metal atoms. The reference elements in our EXAFS experiments were Fe and Cu having *K*-edges of 7112.0 and 8979.0 eV, respectively.

In order to optimize the measurement procedure, the specified data collection interval was divided into three segments: the pre-edge region (from -170 to -20 eV), the near-edge segment (-20 ÷ 80 eV), and EXAFS oscillations area (80 ÷ 800 eV). In the first segment the data were measured with steps of 10 eV, the step was ~ 0.5 eV in near-edge region, and the last segment was scanned with equidistant step 0.05 $Å^{-1}$ on a scale of k – photoelectron momentum. The measurement exposure time T in EXAFS area increased depending on point number n quadratically as ($T = a \cdot n^2 + c$), to compensate for decrease in the EXAFS oscillation amplitude with increasing energy. The constants a and c of this expression were chosen so that the initial exposure for 2 sec at the end of the segment increased to 8 sec. Thus, each spectrum was measured for *ca.* 30 min.

The objects investigated by EXAFS. The list of samples studied by EXAFS is presented in Table 1. Studies on $Fe(OTf)_3 \cdot 6HH$ and $Fe(OTf)_3 \cdot 6DH_2$ are auxiliary and that is why the results are presented in Supplementary Materials. The samples of liquids for EXAFS measurements were prepared in two ways. In the first case, a drop of liquid deposited on an ashless paper filter. This filter was folded in several layers (2-6) to get the absorption jump value $\Delta(\mu d)$ close to unity. In the second case, self-sustaining film was formed due to surface tension in the hole made in substrate foil (aluminum). The magnitude $\Delta(\mu d)$ of the absorption jump in this case was controlled by selecting the thickness of foil. Due to low vapor pressure of IL, DES or LTTM, drying and noticeable change in the film thickness of the sample during the measurement period was not observed.

EXAFS data analysis. Processing of EXAFS data was performed using IFEFFIT[46,47] package, version 1.2.11c. The data were first processed by ATHENA program of this package to fit and subtract their complex background, to normalize the absorption spectrum by unity jump and then to separate the oscillating part of the spectrum – an X-ray absorption fine structure (XAFS). The fine structure extracted in such a way was used for further structural analysis.

The parameters of the local structure of liquid around the resonantly absorbing (reference) atom were determined and refined by fitting the theoretical EXAFS spectrum calculated for selected hypothetical model of the structure to experimental one. This refinement was carried out by ARTEMIS program, version 0.08.014 from the IFEFFIT package and conducted in direct space R, using the phase and amplitude of electron scattering calculated with aid of FEFF 8.20.19 program.

Depending on the spectrum complexity, calculations were carried out either in approximation of one coordination sphere and single scattering of electrons, or by using two or three coordination spheres.

Such a modeling allows refinement of distance from the absorbing atom to the nearest neighbors R_j; the root–mean–square deviation in bond distances between atom pairs σ_j^2 accounting for thermal vibration and statical local disorder[48]; the central atom coordination numbers N_j relative to the nearest neighbors. The threshold energy E_0 of the photoelectron impulses relative to the K absorption edge was also refined. The amplitude reduction factor S_0^2 present in the main EXAFS equation was set to 0.8 so that to exclude its correlation effect on the defined coordination numbers.

Results and discussion

Results of structural analysis by EXAFS

Choise of the S_0^2 coefficient value. The value and oscillation mode of EXAFS signal are dependent on the scattering ways of photoelectron ejected at the X-quantum absorption and on the types of atoms surrounding the resonantly absorbing central metal atom, that is local structure of the studied sample. However, along with photoelectron energy loss at the cost of scattering on atoms of coordination environment, additional energy loss on excitation of all the system of electrons of the studied sample (multielectron excitation) is also possible. By now a complete theory accounting for this effect is absent, that is why an empirical coefficient S_0^2 also named as passive electron decrease in EXAFS signal has been included to the main EXAFS equation by Rehr and Albers[49]. This coefficient serves for quantitative fitting of the theoretically calculated EXAFS amplitudes to experimental ones. The role and physical sense of the S_0^2 coefficient was widely discussed.[48–53]

Choice of the value of S_0^2 coefficient is very important for structural analysis using EXAFS. The "proper" S_0^2 value was considered in details by Campbell *et al*[51]. It was

concluded that the effect of multielectron excitations caused by a photoelectron in the course of EXAFS is negligible, the most probable S_0^2 value is 0.9 with possible deviations of several percents. It was also calculated that the S_0^2 value depends only slightly on the electron's energy and scattering pathway, that is, it is almost equal for all the pathways of electron scattering and all EXAFS spectra. J. Rehr, one of elaborators of analysis of EXAFS spectra, considers[48–53] that in the absence of adequate theory describing the S_0^2 coefficient, it should be approximated by a constant 0.9 ± 0.1 (see also http://millennia.cars.aps.anl.gov/pipermail/ifeffit/2002-October/000155.html).

Due to a correlation coefficient between S_0^2 and coordination numbers N_j in the EXAFS equation being almost equal to one, it is impossible to determine N_j value properly, if the S_0^2 value is unknown. It should be noted that the amplitude reduction coefficient value practically does not have any effect on statistical characteristics of fitting and the radii of coordination spheres (Table 2, R_f and R) but significantly changes N_j values.

In order to justify the choice of S_0^2 value, we used its refinement in EXAFS IL model with the known and fixed coordination numbers, namely, Fe1 IL sample – 1-butyl-3-methylimidazolium tetrachloroferrate(III) ($C_4H_9NC_3H_3NCH_3$)[$FeCl_4$]. The EXAFS spectrum of this IL is well approximated by a simple model of single scattering with one coordination sphere consisting of exactly four Cl atoms. The refinement data for the basic sample at various fixed S_0^2 values are given in Table 2. As can be seen, coordination number N = 4 for Fe atoms is attained at S_0^2 ~ 0.8 and at the higher N values S_0^2 appears to be significantly underestimated.

Refinement of the model at the fixed N = 4 gave S_0^2 = 0.8 ± 0.08. That is why for other studied samples we used S_0^2 = 0.8 in model refinement and N_j determination.

EXAFS of $Cu(CF_3SO_3)_2{\cdot}6H_2N(CH_2)_2OH$, and $Cu(CF_3SO_3)_2{\cdot}6HN(CH_2)_6OH$. These studies helped to understand formation of complexes of copper atoms in solutions of aminoalcohols. As the local structure model for $Cu(OTf)_2{\cdot}6EH$ and $Cu(OTf)_2{\cdot}6HH$ samples was complicated beginning from the one sphere model, the best correspondence with the experimental EXAFS data characterized by statistical R_f criterion was attained using three coordination spheres containing N and C atoms as shown in Table 3. Supposing S_0^2 = 0.8 and a model with three coordination spheres, coordination number of amino groups around Cu atom is between 3.0 and 4.0 for both samples, but somewhat larger for $Cu(OTf)_2{\cdot}6EH$ sample; in this case coordination mode with two chelate metallocycles consisting of five atoms and providing coordination number 4 can be expected. In the case of $Cu(OTf)_2{\cdot}6HH$ sample, chelating is less probable due to the ligand length, and amino alcohol molecules seem to be monodentate ligands with the N-donating atoms, because affinity of Cu atoms to the amino groups is higher than to the hydroxyl groups.

According to Table 3, coordination number of copper atom in $Cu(OTf)_2{\cdot}6EH$ and $Cu(OTf)_2{\cdot}6HH$ samples does not exceed 4, but co-existence of complexes with three and four-coordinated copper atoms cannot be ruled out.

Table 2. EXAFS model parameters *versus* the amplitude reduction factor S_0^2 for a sample with the known coordination number of chlorine atoms (N_{Fe}) in the metal atom environment.[(i)]

Sample	S_0^2	E_0, eV	Scattering path	N_{Fe}	R, Å	σ^2, Å²×10^{-3}	R_f,%
Fe1	1.0	3.1 ± 1.2	Fe-Cl	3.2 ± 0.31	2.204 ± 0.005	3.3 ± 0.6	1.75
Fe1	0.9	3.1 ± 1.2	Fe-Cl	3.5 ± 0.34	2.204 ± 0.005	3.3 ± 0.6	1.75
Fe1	0.8	3.1 ± 1.2	Fe-Cl	4.0 ± 0.4	2.204 ± 0.005	3.3 ± 0.6	1.75
Fe1	0.8 ± 0.08	3.1 ± 1.2	Fe-Cl	4.0	2.204 ± 0.005	3.3 ± 0.6	1.75

[(i)] Calculations were performed using the rectangle window weighting functions (Fig. 1) of width 2.000–14.000 Å^{-1} and 1.000–2.450 Å in the impulse k space and direct R space, respectively. Parameters fixed at fitting are given in semi-bold. The EXAFS spectrum of basic sample was obtained at the same station by the same method and treated by the same procedure as the spectra of all samples studied in this work. That is why we used the S_0^2 coefficient obtained for the basic sample for approximation of the amplitude reduction factor for all the studied samples.

Table 3. The local structure parameters of samples with Cu cation[(ii)]

Sample, model	Scattering pathway	N_j	R, Å	σ², Å²×10-3	R_f, %
$Cu(OTf)_2$·6EH, 3 spheres	Cu–(N/O)	3.6 ± 0.34	2.014 ± 0.006	4.8 ± 0.8	2.0
	Cu–C1	1.35 ± 0.6	2.78 ± 0.03		
	Cu–C2	1.46 ± 0.7	2.97 ± 0.04		
$Cu(OTf)_2$·6HH, 3 spheres	Cu–(N/O)	3.3 ± 0.3	2.025 ± 0.007	4.8 ± 0.8	2.17
	Cu–C1	1.3 ± 0.6	2.98 ± 0.04		
	Cu–C2	0.9 ± 0.5	2.73 ± 0.04		

(ii) Calculations were performed at approximation of the amplitude reduction factor by S_0^2 constant = 0.8 with the rectangle window weighting functions (Fig. 1) 2.000–14.000 Å^{-1} and 1.0–3.0 Å in width in impulse k and direct R spaces, respectively. For nitrogen and carbon atoms in the considered coordination spheres, σ^2 factors are supposed to be equal.

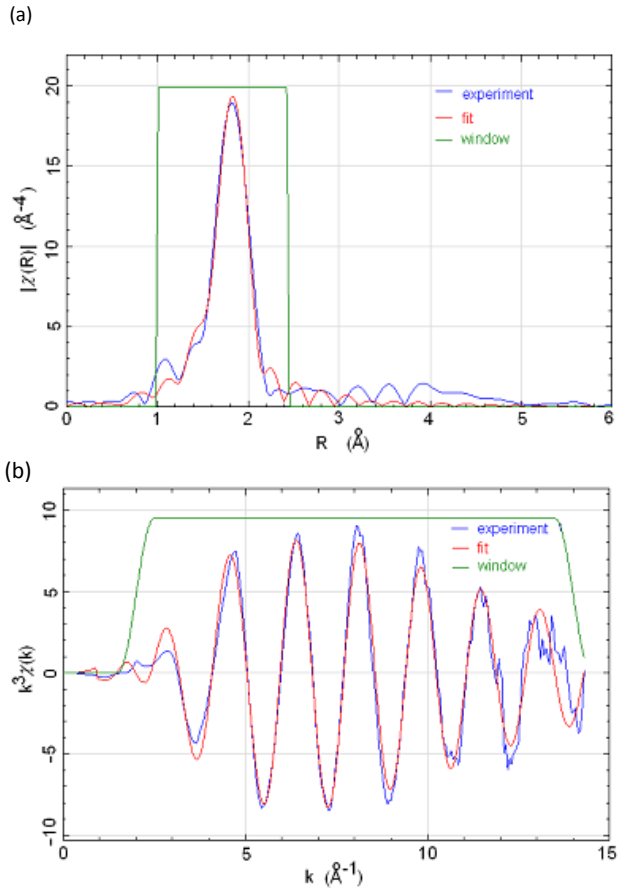

Fig. 1. Fitting of EXAFS spectrum of Fe1 IL $(C_4H_9NC_3H_3NCH_3)[FeCl_4]$ by a single-sphere model with N = 4 and single photoelectron scattering *via* Fe–Cl pathway in (a) metrical *R* and (b) wave *k* spaces. Weighting functions are depicted in green, S_0^2 being 0.8 ± 0.08.

EXAFS of $Cu(CF_3SO_3)_2$·6HN$((CH_2)_2OH)_2$.

Metallocycles were found[9] in the crystal structure of $[Cu\{NH(CH_2CH_2OH)_2\}\{NH(CH_2CH_2OH)(CH_2CH_2O\}]CF_3SO_3$ = $[CuDH_2DH]OTf$. It is pertinent to remind that coordination polyhedron of Cu atom in these crystals is tetragonal bipyramide with coordination number 4 + 2 typical of copper complexes.

However, our results indicate that coordination number of Cu atom in liquid preparation $Cu(OTf)_2$ · 6DEA is not more than 4 (Table 4). Taking into account the above mentioned data, hereafter we shall use a formula $[Cu^{2+}DH_2(DH^-)][(DH_2)_4H^+](OTf^-)_2$ instead of $Cu(OTf)_2 \cdot 6DH_2$.

Volatility of DEA and its mixtures

DH_2 as an individual compound was subjected to thermogravimetry with the simultaneous measurement of the mass spectra of exit vapors and gases. Many DH_2 fragments including water vapor are evolved in the range 200–250°C (Fig. 2), indicating not only DH_2 decomposition but possibly its condensation reaction. The latter reaction can yield a number of products including dimers N,N,N-tris(hydroxyethyl)-ethylendiamine and N,N-bis(hydroxyethyl)piperazine detected at DH_2 heating to 250°C.[55]

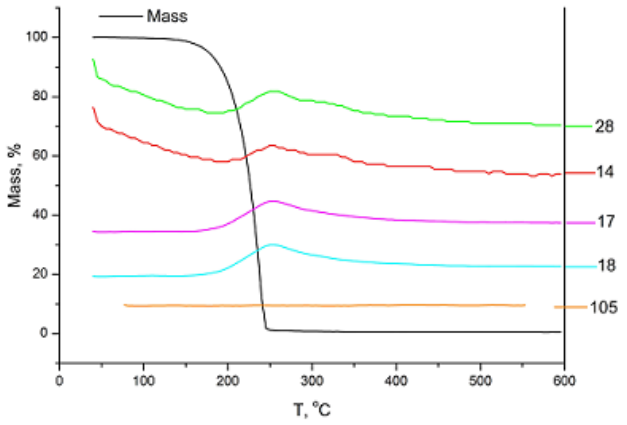

Fig. 2. TGA curve of individual DH_2 and the simultaneously recorded mass spectra of exit vapors and gases.

Mass spectra indicate that DH_2 does not vaporize (Fig. 2). Thus, various reactions proceed in the course of TGA, and this means that method of study has a fatal effect on the studied system and its results should not be used for conclusion about non-volatility of DH_2 in MetILs.

DH_2 was unambiguously detected when $[Cu^{2+}DH_2(DH^-)][(DH_2)_4H^+]$ $(OTf^-)_2$ preparation was studied by MALDI spectrometry (Supplementary Materials, Fig. S3); this possibly came from laser knocking of DEA molecules without heating of substance.

To study the proton effect on the properties of $[Cu^{2+}DH_2(DH^-)][(DH_2)_4H^+ (OTf^-)_2$, we prepared and studied additional preparations, the first of them being $[DH_3^+]OTf^-$. Amine alcohols form crystalline ammonium salts with strong acids. DSC curves presented in Fig. 3(a) indicate that $[DH_3^+]OTf^-$ is a typical ionic liquid.

For comparison, DSC curve of DH_2 is presented in Fig. S4 (Supplementary Materials). Both DSC curves (Figs. S4 and 3(a)) do not exclude possible formation of eutectic in a pseudobinary system $[DH_3^+]OTf^- – DH_2$ (DES formation).

Usually DES consist of ammonium salts and H-bond acceptors in molar ratio 1:2, that is why we prepared the second additional preparation $[(DH_2)_3H^+]OTf^-$ to check possible formation of eutectic.

Table 4. The local structure parameters of samples containing DH_2 ligand. Calculations performed for $S_0^2 = 0.8$, fitting in the range $k = 2–12$ Å^{-1}, $R = 1.2–3.2$ Å

Sample	S_0^2	Scattering pathway	N_j	R, Å	σ^2, Å^2 ×10^{-3}	R_f, %
$Cu(OTf)_2 \cdot 6DH_2$	0.8	Cu-(N/O)	3.0 ± 0.6	1.99 ± 0.01	1.1 ± 1.5	5.1
		Cu-C	2.2 ± 1.8	2.84 ± 0.03	2.0 ± 7.0	

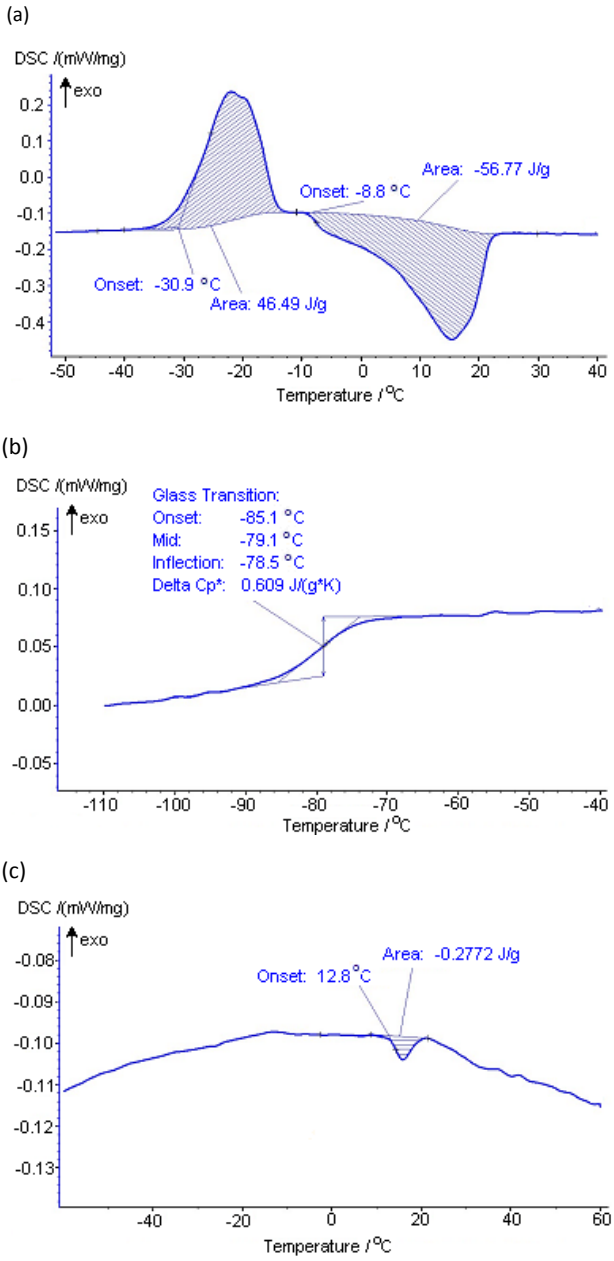

Fig. 3. DSC curves of additional preparations: a) $[DH_3^+]OTf^-$ heating; b) $[(DH_2)_3H^+]OTf^-$ cooling; c) $[(DH_2)_3H^+]OTf^-$ heating.

DSC heating and cooling curves of this preparation are presented in Figs. 4(b) and (c), respectively. In the absence of exothermic extremum of cold crystallization, the endothermic extremum on heating curve of the cooled preparation can be interpreted as transfer from the glassy state of the mixture to plastic one, which is typical of amorphous systems. Thus, we failed to detect eutectic and thus assign $[DH_3^+]OTf^- – DH_2$ system to DES.

The studied system differs in acidic residue from the most existing DES. Chloride ions surrounded by envelope of H-bond donor molecules are typically used in DES, whereas in $[DH_3^+]OTf^- – DH_2$ system acidic residue belongs to a super acid and thus is a very weak base, which hardly forms hydrogen bonds and does not need in the isolating envelope because of a weak interaction with a proton. In $[DH_2^+]OTf^- – DH_2$ system, proton can localize on the N or O atoms of DH_2 molecules, but N atoms are preferential, because proton affinity of N atoms in amine molecules is higher than that of O atoms in alcohol molecules.[40]

Accounting for the aforesaid, $[(DH_2)_3H^+]OTf^-$ preparation should be assigned to low-transition-temperature mixtures[6] (LTTMs) rather than to DES. We studied the third additional preparation, $[(DH_2)_4H^+]OTf^-$, because $[Cu^{2+}DH_2(DH^-)][(DH_2)_4H^+](OTf^-)_2$ preparation can be presented as a solution of crystalline phase $[Cu^{2+}DH_2(DH^-)]OTf^-$ in liquid phase $[(DH_2)_4H^+]OTf^-$.

The IR spectrum of the latter preparation shown in Fig. 4 surprisingly coincides with IR spectrum of $Cu(OTf)_2 \cdot 6DEA$[2] (see Fig. S1b).

In the absence of copper atoms in $(DH_2)_4H^+OTf^-$ preparation, shifts of the IR bands should be rationalized by protonation of the amine and hydroxyl groups of DEA.

Thermogravimetric study of this preparation combined with mass spectroscopy showed that DEA does not vaporize, but in contrast to DH_2, $(DH_2)_4H^+OTf^-$ decomposes in two stages (Figs. 5 and S5 of Supplementary Materials): about 280°C only water vapor is evolved; this fact indicates

that DH_2 molecules condense without decomposition, and various DH_2 fragments are evolved at 410°C.

So, protonation of DH_2 amine and possibly hydroxyl groups results in a noticeable change in the pathway of DH_2 condensation and decomposition in $(DH_2)_4H^+OTf^-$ as compared with pure DH_2 (possibly due to acidic catalysis). Decomposition temperature 410°C at atmospheric pressure corresponds with decomposition temperature of many ILs including $DH_3^+OTf^-$. Mass loss of $(DH_2)_4H^+OTf^-$ preparation at heating to 360°C (Fig. 5) corresponds with a loss of three DH_2 mole fractions of four.

The DH_2 condensation products seem to vaporize without decomposition, because they contain less atom groups able to form H-bonds. This can compensate for vaporization temperature increase inevitable on molecular mass increase and that is why DH_2 condensation products can vaporize without decomposition in contrast to DH_2.

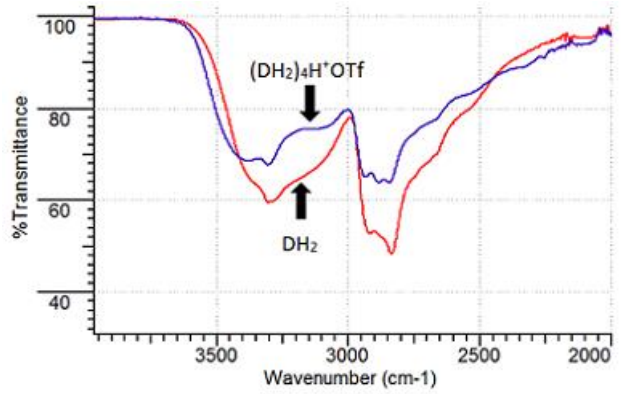

Fig. 4. IR spectrum of $(DH_2)_4H^+OTf^-$ preparation compared with that of DH_2.

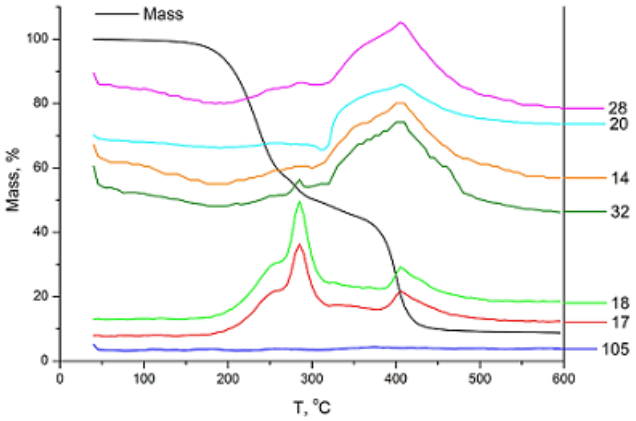

Fig. 5. TGA curve of $(DH_2)_4H^+OTf^-$ preparation and the simultaneously recorded mass spectra of exit vapors and gases.

$[Cu^{2+}DH_2(DH^-)][(DH_2)_4H^+](OTf^-)_2$ preparation was subjected to TGA and mass spectroscopy (Fig. 6). As can be seen, there are three waves of DH_2 decomposition products release including water vapor in the absence of DH_2 vaporization. Three waves of decomposition possibly indicate existence of three different kinds of DH_2 molecules in $[Cu^{2+}DH_2(DH^-)]$ $[(DH_2)_4H^+](OTf^-)_2$ preparation: coordinated to Cu^{2+} ions, protonated and non-bound ones.

Analogous to Fig. 5, the first wave water vapor (not decomposition products) release at ~230°C, can be assigned to condensation of protonated DH_2 molecules. The second wave of water vapor release (320°C) can be considered as a result of condensation of DH_2 molecules coordinated to Cu(II) ions, because no water vapor was detected in other preparations at 320°C. Condensation reaction at this temperature can be catalyzed by Cu(II) ions[56]. Both condensation waves are not accompanied by release of products of DH_2 thermolysis. At last, a distinct third wave (410°C) of decomposition products release corresponds with thermolysis of IL $[DH_3^+]OTf^-$ marked in Fig. 5.

Comparing the properties of DES and LTTM with those of $(DH_2)_4H^+OTf^-$ preparation, let us note their similarity and difference. Analogous to DES[57] or LTTM[6], $(DH_2)_4H^+OTf^-$ has the decreased volatility and increased thermal stability. Similar to DES, it is immiscible with aprotic liquids (e.g., $(DH_2)_4H^+OTf^-$ is immiscible with acetonitrile). However, $(DH_2)_4H^+OTf^-$ does not have eutectic (the presence of eutectic is a basic property of DES) and that is why should be assigned to LTTM. Nonetheless, thermal decomposition of $(DH_2)_4H^+OTf^-$ (Fig. 5) indicates that non-protonated DH_2 molecules are absent in this preparation. In the opposite case, we would observe at least partial decomposition of DH_2 similar to that depicted in Fig. 2. Besides this, the IR spectrum of $(DH_2)_4H^+OTf^-$ preparation indicates that not only amino groups but also hydroxyl groups of DH_2 are protonated. Thermochemical[58–59], acoustic[60] and dielectric[61] studies of mixtures of amines and alcohols demonstrated that H-bonds of N···H–O–R type between amine and alcohol molecules are formed in these mixtures.

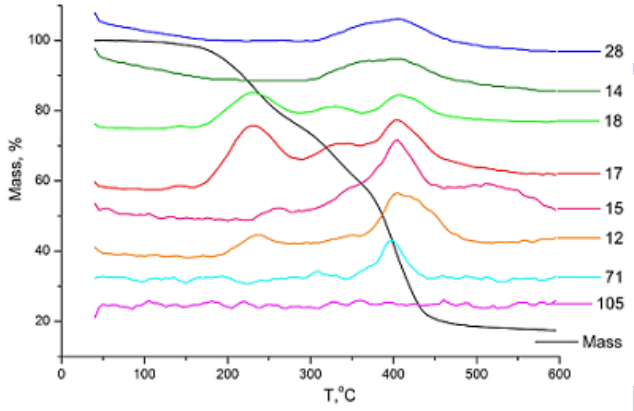

Fig.6. TGA curve of $[Cu^{2+}DH_2(DH^-)][(DH_2)_4H^+](OTf^-)_2$ preparation and the simultaneously recorded mass spectra of exit vapors and gases.

H-bonds are also formed between the strongly polarized N–H bonds of ammonium ions[62] and the oxygen atoms of hydroxyl groups[63–64]. In $(DH_2)_4H^+OTf^-$ preparation containing both ammonium ions and hydroxyl groups, multiple H-bonds exist in the presence of a super acid[26, 39]; these H-

bonds can join hydroxyl and amine groups of DH_2 with mobile positive charges (but not protons themselves) *via* the soliton mechanism (Fig. 7). Such possibility is supported by arguments given in [35, 65]. This mechanism provides mobility of positive charges at the relative immobility of H nuclei over the entire volume of preparation via exchange of σ-bonds and hydrogen bonds: O–H…N↔O…H–N. Due to this exchange, in $(DH_2)_4H^+OTf^-$ preparation there is no separation for DH_3^+ ammonium ions (corresponding with $H_2N^+[(CH_2)_2OH]_2$) and DH_2 molecules, necessary for existence of eutectic, but there works a mechanism of mutual transformation of DH_3^+ ions and DH_2 molecules.

Thus, the properties of $(DH_2)_4H^+OTf^-$ preparation are similar to those of LTTM.

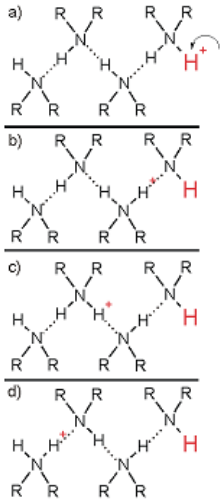

Fig. 7. Scheme of proton charge transfer via the soliton mechanism.

Such solvents deserve particular attention as media for electrochemical processes: scrap utilization, electrolysis, electropolishing and separation of metals[66–69] and also in flow accumulators[7–10].

Conclusions

The studied copper preparation, $[Cu^{2+}DH_2(DH^-)][(DH_2)_4H^+](OTf^-)_2$, is a solution of complex salt $[Cu^{2+}DH_2(DH^-)]OTf^-$ in LTTM with composition $[(DH_2)_4H^+]OTf^-$. Coordination number of metal atoms in $[Cu^{2+}DH_2(DH^-)]OTf^-$ of this solution does not exceed 4, but that in $Fe(OTf)_3 \cdot 6DH_2$ preparation is equal to 6 (See Supplementary Materials); this means that the structural distinction between two preparations similar in composition requires further investigation.

Volatility and decomposition of DH_2 change noticeably on addition of even small amount of acid, and this can be rationalized by the soliton mechanism of positive charge transfer over all the volume of DH_2, giving rise to integration of all DH_2 molecules into a collective cation. DH_2 vaporization also depends on addition of metal salts: addition of iron(III) triflate causes vaporization of DH_2 remaining after DH_2 condensation reaction in the range 300–400°C (see Supplementary Materials), however, in the presence of copper(II) triflate DH_2 does not vaporize but decomposes, although not in the same manner as pure DH_2 does.

Acknowledgements

The authors acknowledge Professor Alexander V. Yatsenko from Department of Chemistry, Lomonosov Moscow State University for fruitful discussions and attention to this work. This study was supported by Lomonosov Moscow State University Program of Development.

References

1 A. P. Abbott, G. Capper, D. L. Davies, R. K. Rasheed and V. Tambyrajah, *Chem. Commun*., 2003, **1**, 70–71.
2 M. H. Chakrabarti , F. S. Mjalli , Inas Muen AlNashef, Mohd. Ali Hashim, Mohd. Azlan Hussain, Laleh Bahadori and Chee Tong John Low, *Renewable and Sustainable Energy Reviews*, 2014, **30**, 254–270.
3 D. V. Wagle, H. Zhao and G. A. Baker. *Acc. Chem. Res*. 2014, **47**, 2299−2308.
4 Qinghua Zhang, Karine De Oliveira Vigier, Sébastien Royer and Francois Jérôme. *Chem. Soc. Rev*., 2012, **41**, 7108-7146.
5 E. Durand and J. Lecomte, P. *Eur. J. Lipid Sci. Technol*., 2013, **115**, 379–385.
6 M. Francisco, Adriaan van den Bruinhorst and Maaike C. Kroon. *Angew. Chem. Int. Ed*., 2013, **52**, 3074 – 3085.
7 T. M. Anderson, D. Ingersoll, A. J. Rose, C. L. Staiger and J. C. Leonard, *Dalton Trans.*, 2010, **39**, 8609–8612.
8 H. D. Pratt III, A. J. Rose, C. L. Staiger, D. Ingersoll and T. M. Anderson, *Dalton Trans.*, 2011, **40**, 11396–11401.
9 H. D. Pratt III, J. C. Leonard, L. A. M. Steele, C. L. Staiger and T. M. Anderson, *Inorganica Chimica Acta*, 2013, **396**, 78–83.
10 H. D. Pratt III, D. Ingersoll, N. S. Hudak, B. B. McKenzie and T. M. Anderson, *Journal of Electroanalytical Chemistry*. 2013, **704**, 153–158.
11 Y. Yoshida, H. Tanaka, G. Saito, L. Ouahab, H. Yoshida and N. Sato. *Inorg. Chem*., 2009, **48**, 9989-9991.
12 S. Hayashi and H.-O. Hamaguchi, *Chem. Lett*., 2004, **33**, 1590-1591.
13 Y. Yoshida and G. Saito. *J. Mater. Chem.*, 2006, **16**, 1254-1262.
14 R. E. Del Sesto, T. M. McCleskey, A. K. Burrell, G. A. Baker, J. D. Thompson, B. L. Scott, J. S. Wilkes and P. Williams, *Chem. Comm*., 2008, 447-449.
15 A. P. Abbott and K. J. McKenzie, *Phys. Chem. Chem. Phys*., 2006, **8**, 4265-4279.
16 N. R. Brooks, S. Schaltin, K. Van Hecke, L. Van Meervelt, J. Fransaer and K. Binnemans, *Dalton Trans*., 2012, **41**, 6902-6905.
17 S. Schaltin, N. R. Brooks, L. Stappers, K. Van Hecke, L. Van Meervelt and K. Binnemans, *Phys. Chem. Chem. Phys*., 2012, **14**, 1706-1715.
18 P. Hapiot and C. Lagrost, *Chem. Rev*., 2008, **108**, 2238-2264.
19 S. Schaltin, N.R. Brooks, K. Binnemans and J. Fransaer, *J. Electrochem. Soc*., 2011, **158**, D21-D27.

20 N. R. Brooks, S. Schaltin, K. Van Hecke, L. Van Meervelt, K. Binnemans and J. Fransaer, *Chem. Eur. J*., 2011, **17**, 5054-5059.
21 C. W. Davies and B. N. Patel, *J. Chem. Soc. (A)*, 1968, 1824- 1828.
22 R. Tauler, E. Casassas and B. M. Rode, *Inorganica Chimica Acta*, 1986, **114**, 203-209.
23 A. Karadag, V. T. Yilmaz and C. Thoene, *Polyhedron*, 2001, **20**, 635-641.
24 J. Madarasz, P. Bombicz, M. Czugler and G. Pokol, *Polyhedron*, 2000, **19**, 457- 463.
25 K. Majid , R. Mushtaq and S. Ahmad, *E-Journal of Chemistry*. 2008, **5(S1)**, 969-979.
26 C. A. Reed, *Accounts of Chemical Research*. 2013, **46**, 2567–2575.
27 P. Dwards, G. Wilkinson, K. M. A. Malik and M. B. Hursthouse, *J.C.S. Chem. Comm*., 1979, 1158-1159.
28 P. G. Edwards, G. Wilkinson, M. B. Hursthouse and K. M. A. Malik, *J.C.S. Dalton*, 1980, 2467-2475.
29 M. Shahid, Armeen Siddique, Istikhar A. Ansari, Farasha Sama, Sandesh Chibber, Mohd Khalid, Zafar A. Siddiqi and Md. Serajul Haque Faizi, *Journal of Coordination Chemistry*, 2015, **68**, 848–862.
30 J.-N. Feng, Y.-Z. Zhou, H.-J. Zhu and S.-J. Tu, *Z. Kristallogr. NCS,* 2006, **221**, 343-344.
31 J. Blaszczyk , Zhenwei Lu , Yue Li, Honggao Yan and Xinhua Ji, *Cell & Bioscience*, 2014, **4**, 1-13.
32 M. Meepripruk and K. J. Haller, *Acta Cryst.*, 2013, **C69**, 1077–1080.
33 G. E. López, I. Colón-Díaz, A. Cruz, S. Ghosh, S. B. Nicholls, U. Viswanathan, J. A. Hardy and S. M. Auerbach, *J. Phys. Chem.* A, 2012, **116**, 1283-1288.
34 U. Viswanathan, D. Basak, D. Venkataraman, J. T. Fermann and S. M. Auerbach, *J. Phys. Chem.* A, 2011, **115**, 5423-5434.
35 V. Zoete and M. Meuwly, *J. Chem. Phys.*, 2004, **120**, 7085-7094.
36 H. J. Berthold, E. Vonholdt, R. Wartchow and T. Vogt, *Z. Kristallogr. – Crystalline Materials*., 1992, **200**, 225-235.
37 I. Olovsson, *Acta Chem. Scandinavica*, 1960, **14**, 1466-1474.
38 M. V. Vener and N. B. Librovich, *International Reviews in Physical Chemistry*., 2009, **28**, 407–434.
39 C. Knight and G. A. Voth, *Accounts of Chemical Research*., 2012, **45**, 101–109.
40 Bun Chan, Janet E. Del Bene and Leo Radom, *J. Am. Chem. Soc*., 2007, **129**, 12197-12199.
41 T. Fujinaga and I. Sakamoto, *J. Electroanal. Chem*.,1976, **73**, 235-246.
42 S. Ichikawa, I. Tomita, A. Hosaka, and T. Sato, *Bull. Chem. Soc. Jpn.*, 1988, **61**, 513-520.
43 G. V. Fetisov, in *Synchrotron radiation. Structure research techniques of materials*, ed. L. A. Aslanov, Moscow, FIZMATLIT, 2007, ch. 5, pp. 488-579. ISBN 978-5-9221-0805-8 [In Russian].
44 G. Bunker, *Introduction to XAFS: A practical guide to X-ray Absorption Fine Structure*. Cambridge University Press. 2010, 260 p.
45 A. A.Chernyshov, A. A.Veligzhanin and Y. V. Zubavichus, *Nuclear Instruments and Methods in Physics Research Section A: Accelerators, Spectrometers, Detectors and Associated Equipment*, 2009, **603**, 95–98.
46 M. Newville, *J. Synchrotron Rad*., 2001, **8**, 322-324.
47 B. Ravel and M. Newville, *J. Synchrotron Rad.*, 2005, **12**, 537–541.
48 J. J. Rehr, *Radiation Physics and Chemistry*., 2006, **75**, 1547–1558.
49 J. J. Rehr and R. C. Albers, *Phys. Rev.*, 1990, **B41**, 8139-8149.
50 J. J. Rehr and R. C. Albers, *Reviews of Modern Physics,* 2000, **72,** 621-654.
51 L. Campbell, L. Hedin, J. J. Rehr and W. Bardtszewski, *Phys. Rev*., 2002, **B65**, 064107.
52 J. J. Rehr and A. L.Ankudinov, *Radiation Physics and Chemistry*, 2004, **70**, 453–463.
53 J. J. Rehr and A. L. Ankudinov, *Coordination Chemistry Reviews*., 2005, **249**, 131–140.
54 D. Lee, L. Sorace, A. Caneschi and S. J. Lippard, Inorg. Chem., 2001, **40**, 6774-6774.
55 M. L. Kennard and A. Allelsen, *Ind. Eng. Chem. Fundam*., 1985, **24**, 129-140.
56 R. I. Khusnutdinov, A. R. Bayguzina, L. I. Gimaletdinova and U. M. Dzhemilev, *Russian Journal of Organic Chemistry*, 2012, **48**, 1191–1196. © Pleiades Publishing, Ltd., 2012.
57 E. Durand, J. Lecomte and P. Villeneuve, *Eur. J. Lipid Sci. Technol*., 2013, **115**, 379–385.
58 J. Fernandez, M. I. Paz Andrade, M. Pintos, F. Sarmiento and R. Bravo, *J. Chem. Thermodynamics*, 1983, **15**, 581-584.
59 M. K. Duttachoudhury and H. B. Mathur, *Journal of Chemical and Engineering Data,* 1974, **19**, 145-147.
60 A. C. H. Chandrasekhar and A. Krishnaiah, *Phys. Chem. Liq.,* 1988, **17**, 315-321.
61 G. M. Kalamse, P. G. Gawali and Rekha Pande, *International Journal of Chemical Sciences*., 2004, **2**, 426-432.
62 P. A. Hunt, C. R. Ashworth, R. P. Matthews. Hydrogen bonding in ionic liquids. // Chem. Soc. Rev. 2015, **44**, 1257-1288 .
63 S. V. Bogatkov, V. N. Romashov, N. I. Kholdyakov and E. M. Cherkasova, *Zhurnal Obshchei Khimii*, 1969, **39**, 266-268.
64 A. P. Ligon. *J. Phys. Chem. A*, 2000, **104**, 8739-8743.
65 Xiao Feng Pang, *Progress in Biophysics and Molecular Biology*., 2013, **112**, 1-32.
66 A. P. Abbott, G. Capper, K. J. McKenzie, and K. S. Ryder, *J. Electroanal. Chem.*, 2007, **599**, 288–294.
67 A. P. Abbott, K. El Ttaib, G. Frisch, K. J. McKenzie and K. S. Ryder, *Phys. Chem. Chem. Phys*., 2009, **11**, 4269–4277.
68 A. M. Popescu, V. Constantin, A. Cojocaru and M. Olteanu, *Rev. Chim*., 2011, **62**, 206–211.
69 E. Gómez, P. Cojocaru, L. Magagnin and E. Valles, *J. Electroanal. Chem*., 2011, **658**, 18–24.